

Molecular geometry of antimalarial amodiaquine in different crystalline environments

Agata Semeniuk ^{*}, Agnieszka Niedospial, Justyna Kalinowska-Tluscik, Wojciech Nitek, Barbara J. Oleksyn

Faculty of Chemistry, Jagiellonian University, ul. R. Ingardena 3, 30-060 Krakow, Poland

Received 8 February 2007; received in revised form 27 March 2007; accepted 31 March 2007

Available online 19 April 2007

Abstract

The crystal structures of antimalarial drug amodiaquine in the form of its free base and two salts, dihydrochloride monohydrate and tetrachlorocobaltate(II), were determined with X-ray single crystal diffractometry. Their conformations and intermolecular interactions are compared to those found in the crystalline amodiaquine dihydrochloride, postulated to contain hydroxyl anion, and in the powder amodiaquine dihydrate dihydrochloride. The molecular structures of the amodiaquine cation and its free base were optimized by the B3LYP calculations and compared to those observed in the crystalline state.

© 2007 Elsevier B.V. All rights reserved.

Keywords: Amodiaquine; Antimalarial; Crystal structure; B3LYP optimization

1. Introduction

Malaria is a very dangerous disease because of which above 1 million people die each year in the world scale [1]. A very serious problem is the resistance built up by malaria parasites, *Plasmodium* sp., against many synthetic drugs in use, especially against chloroquine.

Quite new potential target of the quinoline antimalarials is the enzyme quinone reductase 2 (QR2), which was found in many organisms and also in human red blood cells [2]. The antimalarial drugs most probably could be inhibitors of this enzyme. Amodiaquine was not *explicitly* mentioned in the review about QR2 [3], but the comparison of its molecule to that of 2,6-dichloroindophenol sodium, which is a substrate of QR2, suggests that amodiaquine could serve as an inhibitor of this enzyme.

An important aspect of the processes responsible for the antimalarial activity [4] is the relationship between drug 3D-structure and its antimalarial properties. Crystal struc-

ture analysis of drugs may help in establishing this relationship.

Amodiaquine, 4-[(7-chloro-4-quinolinyl)amino]-2-[(diethylamino)methyl] phenol (see Fig. 1 with atom numbering), belongs to the class of 4-aminoquinolines and is a well known synthetic antimalarial drug against both forms of chloroquine-sensitive and chloroquine-resistant strains of *Plasmodium falciparum*.

The structure of amodiaquine dihydrochloride (ADCh) single crystal was determined for the first time in 1991 by Yennawar and Viswamitra [5]. According to these authors amodiaquine formed a cation with +3 charge, compensated in the crystalline state by one hydroxyl and two chloride anions.

Our results of the structure analysis of the single crystal with the same space group and lattice parameters close to those of ADCh suggest that only two nitrogen atoms, N1 and N3, are protonated and the cation charge is +2. The third nitrogen, N2, covalently binding the H₂N atom, forms an intermolecular hydrogen bond with one of the chloride anions in the unit cell. We show that instead of the hydroxyl anion, postulated by Yennawar and Viswamitra, there is one water molecule, which co-crystallizes with

^{*} Corresponding author. Tel.: +48 12 6632268.

E-mail address: orlow@chemia.uj.edu.pl (A. Semeniuk).

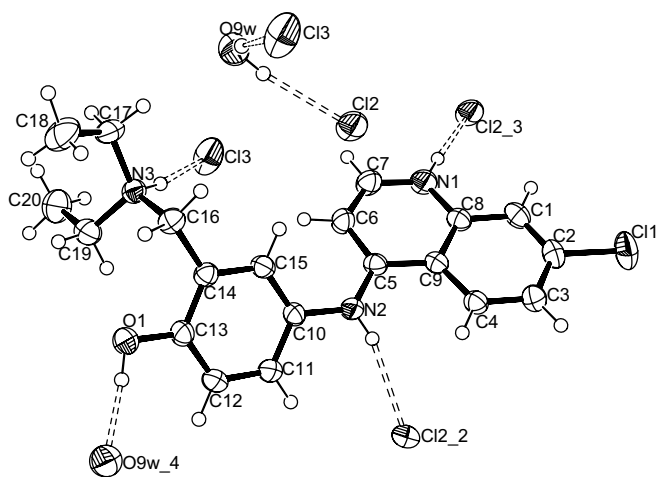


Fig. 1. The asymmetric unit of ADChM with additional water molecule and four chloride anions to show hydrogen bonds. Displacement ellipsoids are drawn at the 50% probability level and H atoms are shown as small spheres of arbitrary radii (ORTEP [9]).

the amodiaquine dihydrochloride and forms its monohydrate (ADChM).

Recently the structure of amodiaquine dihydrate dihydrochloride (ADChD) was determined with powder diffractometry [6]. According to Llinàs et al. [6], in the crystalline ADChD the two protonation sites of the amodiaquinium cation are identical with those found by us. For comparison, the crystal structures of free base amodiaquine (AQ) and of amodiaquine tetrachlorocobaltate(II) (ATChCo) have been determined and described in this paper. The molecular conformations and intermolecular interactions in all four structures are discussed.

Theoretical calculations were performed for the amodiaquine free base molecule and cation in order to optimize the conformations of the isolated species and to compare them with those observed in the crystal and also to consider differences in the partial charges of nitrogen atoms.

2. Crystal structure determination

1. *Amodiaquine dihydrochloride monohydrate (ADChM)* was crystallized by slow evaporation at room temperature from a toluene solution of amodiaquine dihydrochloride dihydrate bought from SIGMA. The diffractometric measurements were carried out for a transparent prismatic crystal of dimensions: $0.38 \times 0.17 \times 0.13$ mm. The crystal data determined in the X-ray experiment are given in Table 1, together with those for amodiaquine dihydrochloride (ADCh) reported by Yennawar and Viswamitra in 1991 [3] and for amodiaquine dihydrochloride dihydrate (ADChD) published by Llinàs et al. [4].
2. *Free base amodiaquine (AQ)* was obtained by mixing amodiaquine dihydrochloride and sodium hydroxide in the form of water solutions. The precipitate was recrystallized by slow evaporation at room temperature from a

propanol solution. Diffraction data were collected for a transparent plate crystal with dimensions: $0.38 \times 0.33 \times 0.05$ mm.

The structure determination based on the results of the experiment at temperature 293 K displayed a disorder of the co-crystallized propanol solvent, so the experiment for the same crystal was performed at 100 K (AQ_100). The crystal data for the AQ and AQ_100 are listed in Table 1.

3. *Amodiaquine tetrachlorocobaltate(II) (ATChCo)* was obtained by mixing alcohol solutions of amodiaquine dichloride and cobalt(II) chloride hexahydrate. Crystallization by slow evaporation at room temperature from an ethanol solution yielded blue crystals of prismatic shape. Diffraction data were collected for a crystal of dimensions: $0.19 \times 0.09 \times 0.05$ mm. Crystal data for ATChCo are given in Table 1.

In all the cases, the phase problem was solved by direct methods and the structure refinement was carried out by full matrix least-squares using SHELXL97 [7]. All hydrogen atoms were found on the difference Fourier maps, but those connected to carbon atoms were placed in calculated positions and refined isotropically, using a riding model.

3. Results of crystal structure analysis

3.1. Amodiaquine dihydrochloride monohydrate (ADChM)

The asymmetric unit of ADChM and the projection of the unit cell along y axis are shown in Figs. 1 and 2, respectively.

Selected bond lengths and bond angles in the amodiaquine cation are listed in Table 2 and compared with those reported in [6] as well as with AQ, ATChCo and calculated values.

The most characteristic torsion angles for all compared molecules are given in Table 3. Since the structures ADChD, ADChM, AQ and ATChCo are centrosymmetric, both enantiomers are present in their unit cells.

The packing of the molecules in the unit cell of ADChM is determined mainly by hydrogen bonding system, parameters of which are presented in Table 4 and Fig. 1.

Thorough inspection of the hydrogen bonds in the crystal structure of ADChM revealed the presence of the water molecule instead of the hydroxyl group reported in [5]. The additional confirmation of the existence of water molecules in the structure of ADChM are channels observed along the direction parallel to $[010]$ (Fig. 2). The channels are filled with water molecules and chloride anions, which are linked *via* hydrogen bonds, $O9W-H9AW \cdots Cl3$, $O9W-H9BW \cdots Cl2$, and form a chain system. The water molecule is also a proton acceptor in the hydrogen bond, $O1-H1 \cdots O9W$, with the amodiaquine hydroxyl group.

Another type of intermolecular interactions is a partial $\pi-\pi$ stacking shown in Fig. 3.

Table 1
Crystal data, measurement and calculation details for six crystal structures of amodiaquine cations and free base

	Amodiaquine dichloride (ADCh) [5]	Amodiaquine dichloride dihydrate (ADChD) [6]	Amodiaquine dichloride monohydrate (ADChM)	Free base amodiaquine (AQ)	Free base amodiaquine (AQ_100)	Amodiaquine tetrachlorocobaltate (ATChCo)
Formula	$C_{20}H_{24}ClN_3O^{3+} \cdot 2Cl^- \cdot OH^-$	$C_{20}H_{24}ClN_3O^{2+} \cdot 2Cl^- \cdot 2H_2O$	$C_{20}H_{24}ClN_3O^{2+} \cdot 2Cl^- \cdot H_2O$	$C_{20}H_{22}ClN_3O \cdot C_3H_8OH$	$C_{20}H_{22}ClN_3O \cdot C_3H_8OH$	$C_{20}H_{24}ClN_3O \cdot CoCl_4$
M (g mol ⁻¹)	446.5	464.8	446.79	415.95	415.95	558.60
Solution	Ethanol	–	Toluene	Propanol	Propanol	Ethanol
Temp (K)	293	298	293(2)	293(2)	100	293(2)
Crystal system	Monoclinic	Monoclinic	Monoclinic	Triclinic	Triclinic	Triclinic
Space group	$P2_1/c$	$P2_1/c$	$P2_1/c$	$P\bar{1}$	$P\bar{1}$	$P\bar{1}$
a (Å)	16.379(6)	7.8387(1)	16.4066(3)	8.8686(3)	8.8119(2)	9.4328(2)
b (Å)	7.714(5)	26.9917(5)	7.7182(1)	11.9454(5)	11.7788(3)	11.2628(2)
c (Å)	17.583(6)	10.8080(2)	17.6179(4)	12.5622(5)	12.0787(3)	12.2787(3)
α (°)	90	90	90	111.387(2)	109.248(1)	87.737(1)
β (°)	107.54(4)	92.963(1)	107.557(1)	103.741(2)	105.084(1)	76.972(1)
γ (°)	90	90	90	104.226(2)	104.189(1)	69.902(1)
V (Å ³)	2119.3	2283.6(2)	2127.02 (7)	1119.50(8)	1064.86(5)	1192.49(4)
Z	4	4	4	2	2	2
D (g cm ⁻³)	1.233	1.352	1.395	1.234	1.297	1.556
$F(000)$	932	976	936	444	444	570
μ (mm ⁻¹)	2.9	0	0.452	0.194	0.204	1.297
Radiation	CuK α	CoK α	MoK α	MoK α	MoK α	MoK α
<i>Data collection</i>						
Diffractometer	Enraf-Nonius CAD4	Stoe linear PSD Debye-Scherrer geometry	Bruker Nonius KappaCCD	Bruker Nonius KappaCCD	Bruker Nonius KappaCCD	Bruker Nonius KappaCCD
h (min), h (max)	–19, 19	–	0, 21	0, 11	0, 11	–12, 12
k (min), k (max)	0, 9	–	–9, 10	–15, 15	–15, 14	–14, 14
l (min), l (max)	0, 12	–	–22, 21	–16, 15	–15, 14	–15, 15
θ min (°)	2.97	1.0	2.38	2.58	2.61	2.48
θ max (°)	27.48	30.0	27.51	27.46	27.44	27.37
n . integrated ref.	8342	392	9208	14098	18189	29597
n . unique ref.	4601	–	4863	5101	4832	5379
Completeness (%)	–	–	99.8	99.5	99.5	99.8
<i>Refinement</i>						
$R1$ for $F_0 > 2\sigma(F_0)$	0.0656	0.037	0.0439	0.0649	0.0437	0.0504
$R1$ for all data	0.0866	–	0.0768	0.1208	0.0595	0.1279
$wR2$ for $F_0 > 2\sigma(F_0)$	0.1757	0.047	0.1051	0.1417	0.1012	0.0855
GoF on F_2	1.045	–	1.037	1.050	1.078	1.000

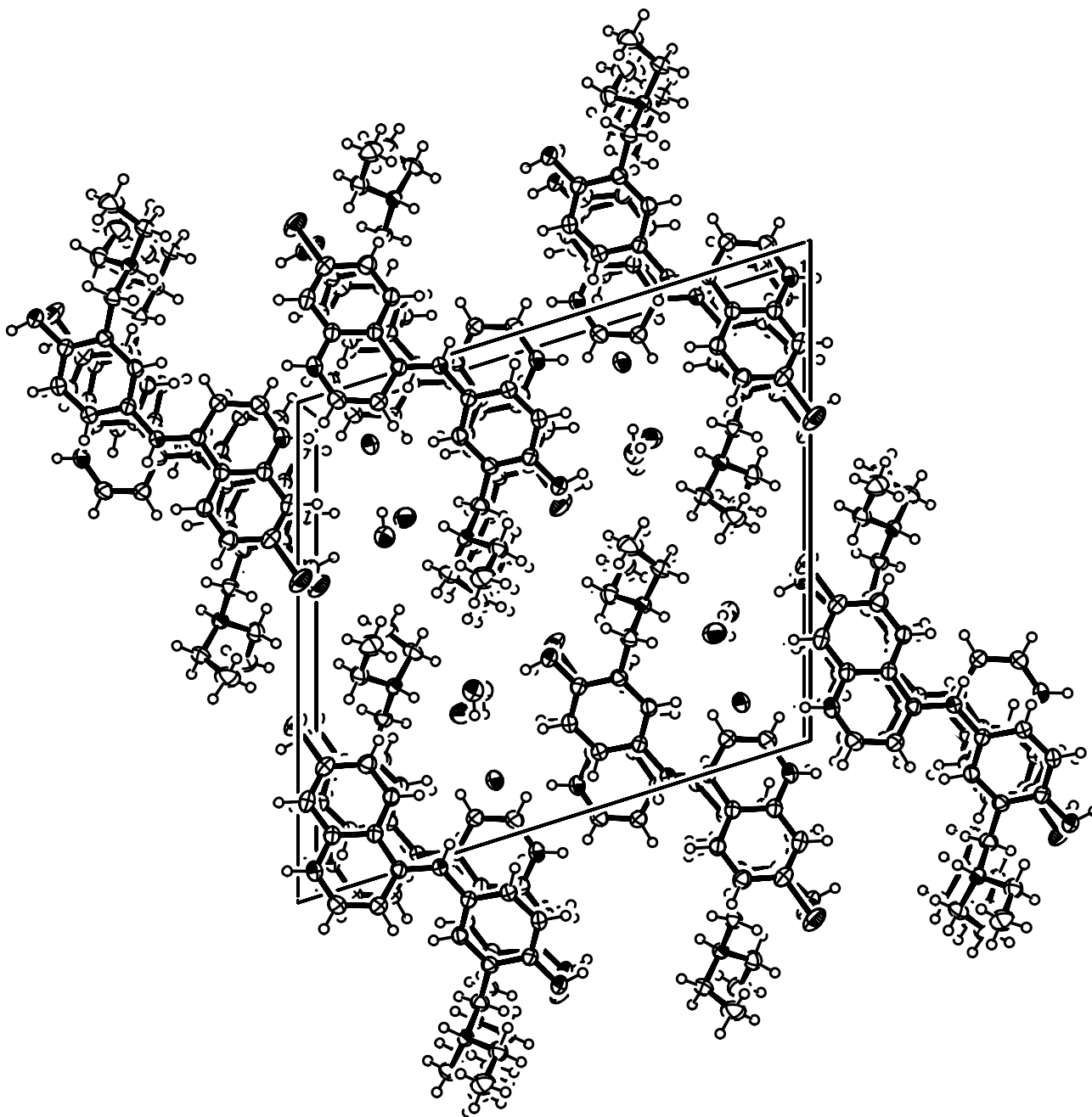


Fig. 2. Projection of the unit cell of ADChM along y axis.

This interaction can be inferred from the mutual positions of the benzene ring, C10–C15, of one molecule and the part of the quinoline ring containing the Cl substituent of another molecule ($-x + 1, y + 0.5, z + 0.5$). The smallest distances between the interacting moieties are in the range of 3.426(2)–3.585(2) Å while the angle between quinoline and benzene ring planes is about 9° [8].

3.2. Free base amodiaquine (AQ)

The asymmetric unit of AQ₁₀₀ is shown in Fig. 4.

The packing of the molecules in the unit cell of amodiaquine free base is determined by the hydrogen bonding system, parameters of which are presented for both temperatures in Table 5 and Fig. 4.

The interactions *via* π – π stacking occur between the quinoline moieties related by inversion centres. The closest atoms of two interacting rings are C2 and C7 ($-x + 1, -y, -z + 1$), their distance being 3.343(2) Å (Fig. 5). Moreover, the chain system formed by amodiaquine and solvent molecules, connected by hydrogen bonds N2–H2N \cdots O2 and O2–HO2 \cdots N1, is observed along [100] direction. There is one intramolecular hydrogen bond, O1–HO1 \cdots N3,

Table 2
Selected parameters for the experimentally determined and optimized molecular structures

	ADChM	ADChD [6]	AQ	AQ_100	ATChCo	Optimized	
						AQ cation	AQ free base
C7–N1	1.333(3)	1.318(2)	1.320(3)	1.327(2)	1.332(4)	1.344	1.321
C8–N1	1.371(3)	1.368(2)	1.369(3)	1.371(2)	1.373(4)	1.381	1.365
C7–N1–C8	121.2(2)	119.7(1)	116.0(2)	116.3(1)	121.9(3)	122.00	116.06
C5–N2	1.347(2)	1.366(2)	1.369(3)	1.365(2)	1.338(4)	1.355	1.378
C10–N2	1.417(2)	1.398(2)	1.418(3)	1.418(2)	1.419(4)	1.429	1.414
C5–N2–C10	128.7(2)	128.2(2)	125.9(2)	125.3(1)	129.7(3)	127.99	126.84
C5–N2–H2N	114.7(2)	115.1(2)	118(2)	118(2)	116(2)	116.79	115.09
C10–N2–H2N	116.1(2)	115.0(2)	116(2)	117(2)	114(2)	115.19	114.4
C16–N3	1.510(2)	1.54(2)	1.473(4)	1.482(2)	1.496(4)	1.534	1.479
C17–N3	1.504(2)	1.49(2)	1.485(6)	1.482(2)	1.503(4)	1.532	1.475
C16–N3–C17	110.9(2)	109.8(2)	112.1(3)	112.2(1)	112.4(3)	111.52	112.72
C19–N3	1.498(2)	1.49(2)	^a	1.477(2)	1.515(4)	1.524	1.479
C19–N3–C16	112.2(2)	109.7(2)	^a	111.8(1)	112.7(3)	112.84	113.26
C19–N3–C17	113.9(2)	114.6(2)	^a	111.1(1)	112.2(3)	114.02	113.11
C3–C2	1.399(3)	1.42(2)	1.397(4)	1.408(2)	1.397(5)	1.414	1.411
C1–C2	1.359(3)	1.34(2)	1.359(4)	1.366(2)	1.362(5)	1.384	1.373
C3–C2–C1	122.1(2)	123.3(1)	121.7(2)	121.9(2)	121.7(3)	120.72	121.56
C12–C13	1.385(3)	1.401(2)	1.377(4)	1.386(2)	1.379(5)	1.400	1.399
C14–C13	1.403(3)	1.38(2)	1.395(4)	1.406(2)	1.389(4)	1.411	1.412
C12–C13–C14	119.8(2)	118.1(1)	120.2(2)	120.2(2)	120.2(3)	120.16	119.36
Pyramidity (%)	72.78	81.96	–	78.80	71.84	68.42	66.17

^a The parameters for disordered fragment were omitted.

Table 3
Comparison of torsion angles for the investigated structures

Torsion angle (°)		ADChD [6]	ADChM	AQ_100	ATChCo	Optimized	
						AQ-cation	AQ free base
τ_1	C13–C14–C16–N3	–95.8(3)	–93.9(2)	49.0(2)	–64.7(4)	–97.1	42.0
τ_2	C5–N2–C10–C15	46.9(3)	–35.2(3)	–43.1(2)	153.8(3)	–134.3	–47.4
τ'_2	C5–N2–C10–C11	–121.0(3)	151.3(2)	141.9(2)	–32.4(5)	51.5	137.2
τ_3	C6–C5–N2–C10	5.0(3)	–15.7(3)	–15.7(3)	–10.8(5)	11.1	–10.5
	C14–C16–N3–C17	–174.8(3)	–169.4(2)	–175.6(1)	166.1(3)	–161.5	–163.6
	C14–C16–N3–C19	58.4(3)	62.1(2)	58.8(2)	–65.9(4)	68.7	66.4

Table 4
Comparison of hydrogen bonds in the structures of amodiaquine dihydrochloride (ADCh) and amodiaquine dihydrochloride monohydrate (ADChM)

D–H···A	D–H (Å)		D···A [Å]		D–H···A [°]	
	ADCh [5]	ADChM 2005	ADCh [5]	ADChM 2005	ADCh [5]	ADChM 2005
N1–H1N···C12 #1	1.076	0.907(3)	3.067	3.090(2)	171.9	173(2)
N2–H2N···C12 #2	0.767	0.820(2)	3.253	3.260(2)	160.1	159(2)
N3–H3N···C13	1.068	0.943(2)	3.008	3.022(2)	179.4	171(2)
O1–H1···O9W #3	1.048	0.820(2)	2.700	2.708(2)	163.7	172(2)
O9W–H9A···C13 #4	–	0.843(3)	–	3.091(2)	–	171(3)
O9W–H9B···C12	–	0.874(2)	–	3.194(2)	–	169(3)

#1 $-x + 1, -y + 1, -z + 1$; #2 $-x + 1, y + 1/2, -z + 1/2$; #3 $x, -y + 1/2, z - 1/2$; #4 $x, y - 1, z$.

which stabilizes the conformation of the diethylamine moiety.

3.3. Amodiaquine tetrachlorocobaltate(II) (ATChCo)

The asymmetric unit of ATChCo is shown in Fig. 6.

The packing of the molecules in the unit cell of ATChCo is determined mainly by hydrogen bonding system, param-

eters of which are presented in Table 6. The hydrogen atom belonging to N2 is engaged in a weak bifurcated hydrogen bond with C14 #3 and C14 #4 atoms.

The quinoline moieties related by the inversion centre (with coordinates 0.5, 0.5, 0.5) are mutually parallel and partially stacked together, like in the structure of AQ_100. The corresponding atom distances in the parallel rings, which do not contain nitrogen atoms, are comprised

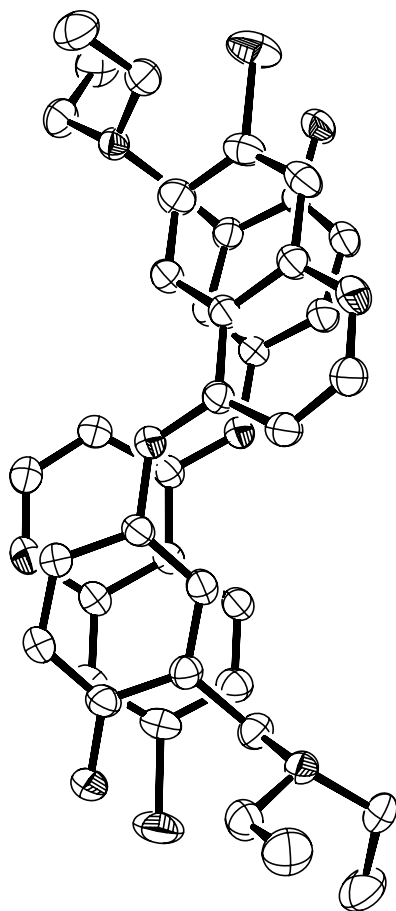


Fig. 3. Partial π - π stacking in the structure of ADChM.

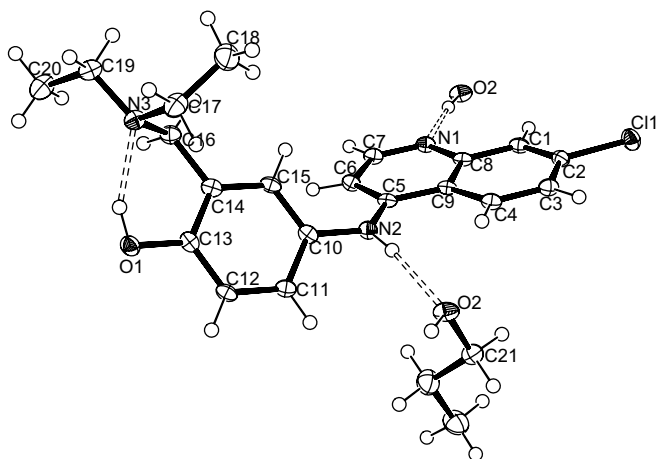


Fig. 4. The asymmetric unit of AQ_100 with the additional solvent molecule to show hydrogen bonds. Displacement ellipsoids are drawn at the 50% probability level and H atoms are shown as small spheres of arbitrary radii (ORTEP [9]).

in the region of 3.502(4)–3.606(4) Å (Fig. 7). The amodiaquine cations and $[\text{CoCl}_4]^{2-}$ anions form chains along [111] direction. The ions are linked *via* hydrogen bonds O1–HO1...Cl2#2, N3–H3N...Cl3#2 and N1–H1N...Cl5#1 (Table 6).

4. Theoretical calculations

Ab initio calculations were performed with the use of Gaussian 2003 [10]. In the first step of the calculations the molecular structures of ADChM and AQ_100, found in the crystal, were fully optimized at the B3LYP/6-31G(d,p) [11–13] level of the theory. In the next step the natural charge distribution was calculated [14].

The optimized cation and free base conformations as well as those observed in the ADChM and AQ_100 crystals are compared in Fig. 8a–d.

The optimal geometries were verified on the minima conditions of frequencies among which no imaginary values were observed. The values of heat of formation and the energy differences between amodiaquine cation and free base, calculated both for the crystalline forms and for the optimized models are shown in Table 7.

Negative values of the energy of protonation: $\Delta E = E_{\text{cation}} - E_{\text{free base}}$, listed in Table 7, suggest that the protonation of free base amodiaquine is a spontaneous process. They are comparable to those obtained for the protonation of aliphatic diamines [15].

5. Discussion

The molecular geometry of amodiaquine depends on its protonation: the immediate surroundings of the two nitrogen atoms, N1 and N3, are different in the free base and in the cations (Table 2).

The most spectacular differences can be noticed in the values of the bond angles with the nitrogen atom in the apex. In the quinoline fragment the protonation of N1 results in certain enlargement of the C7–N1–C8 angle from 116.3(1)° in the free base to 121.2(2)–121.9(3)° in the cations. This change is in agreement with VSEPR theory [16]. According to this theory, certain shift of the lone electron pairs of the nitrogen atoms towards their protons may be inferred from the values of the bond angles C–N–C, which are greater than those observed in non-protonated amines. The influence of the protonation of N3 on the bond angles may be interpreted using the notion of the pyramidity, $P(\%)$ [17]. This parameter describes the distortion of the nitrogen environment from the ideal tetrahedral hybridization. The values of $P(\%)$, given in Table 2, show that the pyramidity of N3 in the free amodiaquine base is higher than those in the cations. The decrease of $P(\%)$ may be treated as a measure of the electron withdrawing properties of the protons linked to the nitrogen atoms. The inspection of the angles C5–N2–C10, H2N–N2–C5 and H2N–N2–C10 (Table 2) shows that the bonds formed by N2 are approximately coplanar. This observation suggests a different behaviour of the N2 atom of in comparison to N3.

The shape of the molecules can be conveniently described by three torsion angles: $\tau_1 = \text{N3–C16–C14–C15}$, $\tau_2 = \text{C15–C10–N2–C5}$ and $\tau_3 = \text{C10–N2–C5–C6}$ (Table 3). The differences in the overall conforma-

Table 5
Comparison of hydrogen bonds in both structures of free base amodiaquine

D—H···A	D—H (Å)		H···A (Å)		D···A (Å)		D—H···A (°)	
	AQ	AQ_100	AQ	AQ_100	AQ	AQ_100	AQ	AQ_100
N2—H2N···O2	0.81(3)	0.82(2)	2.11(3)	2.09(2)	2.917(3)	2.904(2)	169(3)	172(2)
O1—HO1···N3	0.84(4)	0.88(3)	1.95(4)	1.92(3)	2.730(4)	2.736(2)	154(4)	153(2)
O2—HO2···N1#1	0.87(4)	0.84(3)	1.88(4)	1.89(3)	2.738(3)	2.724(2)	169(4)	174(3)

#1 $x + 1, y, z$.

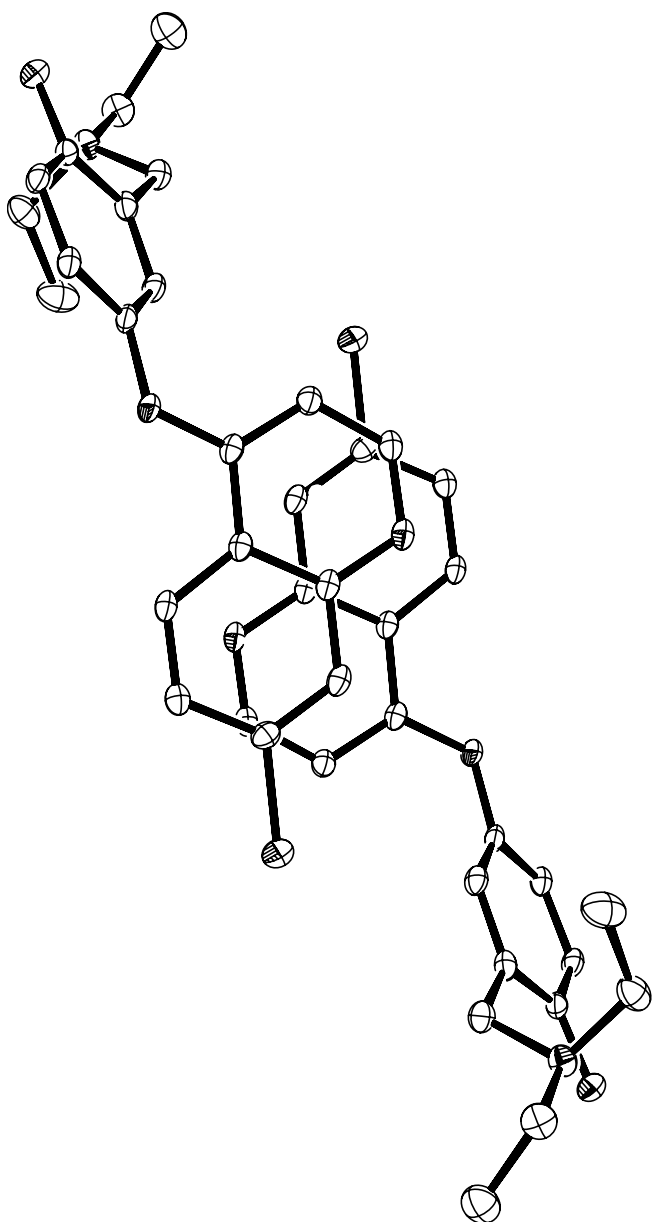


Fig. 5. Partial π – π stacking in the structure of AQ_100.

tion between cations as well as between them and free base may be the result of different hydrogen bonding (Tables 4–6), which in turn depends on protonation of nitrogen atoms and on the presence of co-crystallising ions and molecules.

The conformation characterized by τ_1 and τ_3 (Table 3) is synclinal and synperiplanar, respectively, for all the mole-

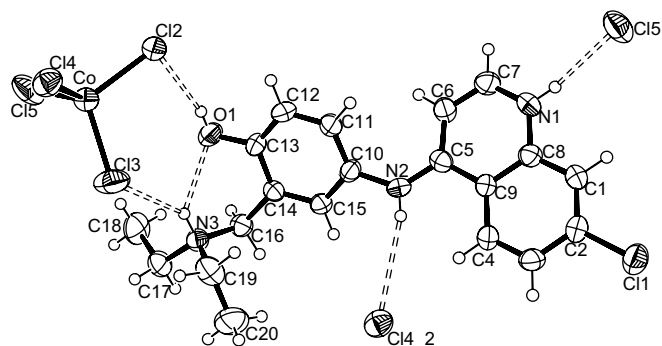


Fig. 6. The asymmetric unit of ATChCo with two additional chlorine atoms to show hydrogen bonds. Displacement ellipsoids are drawn at the 50% probability level and H atoms are shown as small spheres of arbitrary radii (ORTEP [9]).

cules including the optimized conformers of the cation and free base. The angles τ_2 and τ'_2 for the cation in the ATChCo crystal and in the optimized cation differ from those of ADChD, ADChM, AQ_100 and the optimized AQ free base. In consequence, their conformation in respect to τ_2 can be called anticlinal in contrast to the synclinal for the other species.

The absolute values of τ_1 in cations, much greater than those in the free base, seem to result from such orientation of the diethylamino methyl group, which favours the interaction of N3 with C13 *via* hydrogen bond. This observation is in agreement with the behaviour of N3 in ADChD, where the length of N3—H3N···C13 bond is very similar to that in ADChM. On the other hand, formation of the intramolecular hydrogen bond, O1—HO1···N3 (Table 4), in the free base also favours the smaller τ_1 angle.

The values of τ_2 and τ_3 show that in the amodiaquine cation the quinoline moiety and 4-[(7-chloro-4-quinolinyl)amino] phenol fragment are not coplanar, which may be explained by the stereoelectronic effect. This effect consists in competition between the resonance of the quinoline and phenol moieties linked by N2 “bridge” and the tendency to lessen the H6···H15 steric hindrance. This hindrance is also relaxed by the increase of the angle C10—N2—C5. The value of this angle varies from 125.3(1)° for AQ_100 to 129.7(3)° for ATChCo. In ADChD [6] it is 128.2(2)°, also much greater than 120°.

As shown in Fig. 9, the C5—N2 bond length increases with the increase of the torsion angles around N2—C10 bond. This dependence may be explained by the observation that the increase of these torsion angles deteriorates

Table 6
Hydrogen bonds in the structure of amodiaquine tetrachlorocobaltate

D—H...A	D—H (Å)	H...A (Å)	D...A (Å)	D—H...A (°)
N1—H1N...Cl5 #1	0.84(3)	2.35(3)	3.171(4)	167(3)
O1—HO1...Cl2 #2	0.74(3)	2.37(3)	3.096(3)	166(4)
N2—H2N...Cl4 #3	0.77(3)	2.91(3)	3.655(3)	165(3)
N2—H2N...Cl4 #4	0.77(3)	3.34(3)	3.588(3)	102.8(2)
N3—H3N...O1	0.86(3)	2.34(3)	2.916(4)	125(2)
N3—H3N...Cl3 #2	0.86(3)	2.47(3)	3.194(3)	143(2)

#1 $x+1, y, z$ #2 $x, y+1, z+1$ #3 $-x, -y+1, -z+1$ #4 $x, y+1, z$.

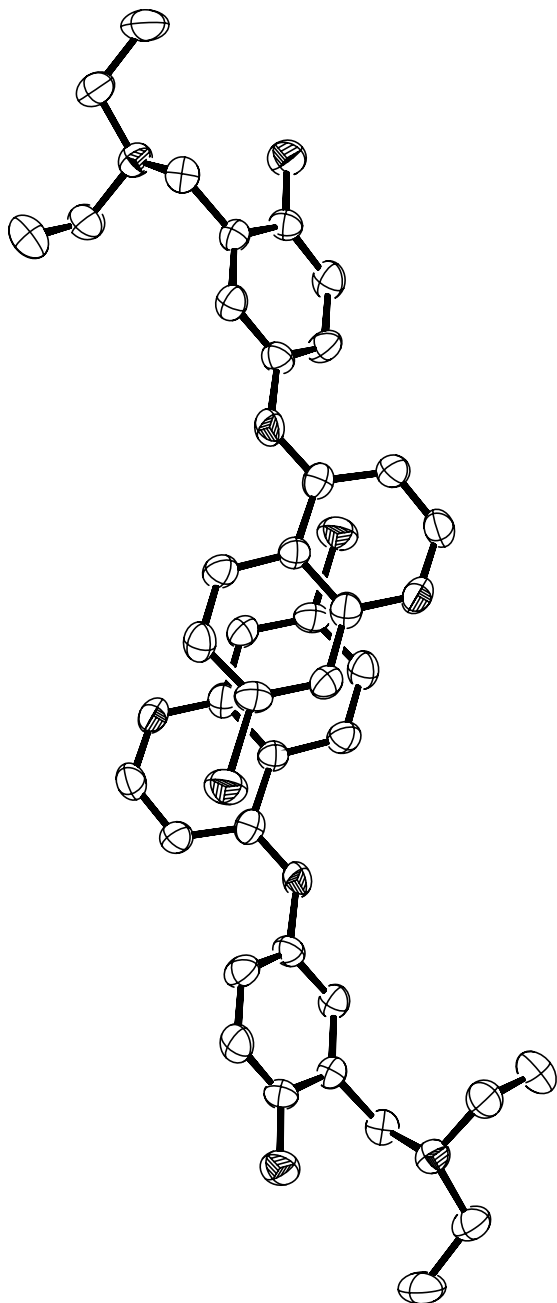


Fig. 7. π – π stacking of ATChCo cations.

the conjugation between the quinoline ring system and the lone electron pair of the N atom, leading to certain elonga-

tion of the C5–N2 bond. Such tendency is in agreement with the results of B3LYP calculations performed by Kortiřová et al. [18] for diphenylamines.

It is worth mentioning that the conformation of the optimized AQ free base molecule is very similar to that observed in the crystal, while the optimized cation adopts the conformation more similar to that observed in the tetrachlorocobaltate salt and different from those observed in the hydrochlorides. This can be probably explained by the greater conformation lability of the cation. It is also possible that the results of calculations for cation may be more sensible to the environment than the results for the free base. It would explain why the optimization performed for the isolated molecules has led, in the case of cation, to the value of the torsion angle C5–N2–C10–C11, which does not match the relationship shown in Fig. 9.

The results of the theoretical calculations are illustrated by superimposition of the quinoline fragments of the molecules in pairs. The pair: cation–free base (Fig. 8a), observed in the crystals, shows a remarkable difference in the orientation of the (diethylamino)methyl moiety (see also torsion angles in Table 3). A similar difference occurs in the pairs: optimized cation–optimized free base (Fig. 8b) and optimized cation–cation observed in the crystal (Fig. 8c), but in both these pairs an additional dissimilarity appears in the orientation of the benzene ring. A remarkable conformation similarity is shown by the pair of the free base molecules, one of them optimized and the other observed in the crystal (Fig. 8d).

Table 8 presents the natural charge distribution (POP=NBO) calculated at the B3LYP/6-31G(d,p) level of theory. All three nitrogen atoms, N1, N2 and N3, have negative charges though N1 and N3 are protonated. On the other hand, the negative charges at the nitrogen atoms, especially those at N3 in the cation, are much smaller than that of the oxygen of the hydroxyl group. The calculated charge of N3 is more positive for the protonated atom in the cation than for the atom N3 with the lone electron pair in the free base. The negative charges of the nitrogen atoms are also similar to those calculated by Kortiřová et al. [18]. The role of π -electron density in the amodiaquine quinoline moiety in the formation of a complex with heme was discussed by Casabianca and de Dios [19]. According to them the ring A, containing the nitrogen atom, is electron-rich while the ring B (without N atom) is electron-poor. The total charges for each of these rings, calculated from the data given in Table 8, suggest the opposite: ring A (charge: -0.23) is electron-poorer than ring B (charge: -0.42).

The intermolecular hydrogen bonds formed by the protonated nitrogen atoms, N1 and N3, as well as by N2–H and –OH groups of cations (Tables 4, 6), are very important from the viewpoint of amodiaquine biological activity. The molecule of free amodiaquine base differs from the cation in the presence of the intramolecular hydrogen bond –OH...N3. The π – π stacking, which also plays a significant role in the drug–receptor interactions occurs in the crystals of all the presented structures. This feature is inter-

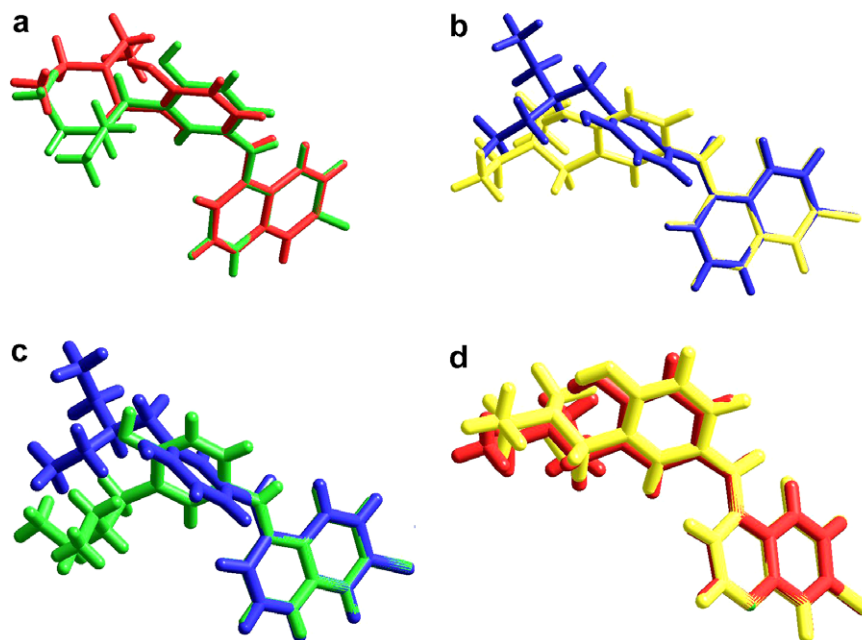


Fig. 8. (a) Superimposition of the quinoline fragment of the cation (green) on the free base molecule (red), both observed in the crystals. (b) Superimposition of the quinoline fragments of the optimized cation (blue) on the optimized free base molecule (yellow). (c) Superimposition of the quinoline fragment of the optimized cation (blue) on the cation observed in the crystal (green). (d) Superimposition the of quinoline fragment of the optimized free base (yellow) on the free base observed in the crystal (red). (For interpretation of the references to colour in this figure legend, the reader is referred to the web version of this article.)

Table 7
Heat of formation (Hartree) calculated for amodiaquine cation and free base.

Heat of formation		In crystal	Optimized	The energy difference (ΔE)	
				(Hartree)	(kcal/mol)
ATChCo (cation)		-1475.39994893	-1475.81900474	-0.41905581	-262.9615
AQ_100 (free base)		-1474.70068010	-1475.10049000	-0.39980990	-250.8845
The energy difference (ΔE)	(Hartree)	-0.69926883	-0.71851474	-	-
	(kcal/mol)	-438.7979	-450.8749	-	-

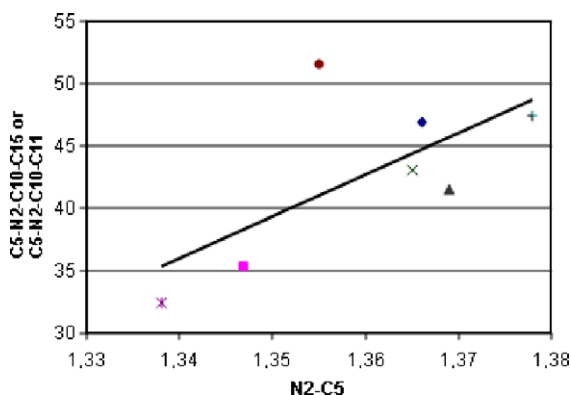


Fig. 9. Scatter plot of the absolute values of τ_2 or τ'_2 as function of bond length N2—C5 (+, optimized free base; •, optimized cation; ▲, AQ; ◆, ADChD; ×, AQ_100; ■, ADChM; ✕, ATChCo).

esting in confrontation with the recent papers by de Dios et al. [20,21], concerning the mechanism of amodiaquine antimalarial activity. According to these authors, the amo-

diaquine molecules may form dimers with the quinoline parts eclipsed with the antiparallel orientation, while in the structures described in this paper they are mutually shifted (AQ_100 and ATChCo) or the stacking occurs between quinoline and benzene rings (ADChM).

6. Conclusions

The X-ray structure analysis of amodiaquine dihydrochloride monohydrate proved the presence of the water molecule instead of the hydroxyl anion in its crystal and changed a previous view concerning the total charge of the amodiaquine cation: it is +2 and not +3, as postulated in [5]. This observation, which has been supplemented with the results of ab initio B3LYP optimization, may help to better understand the mechanism of the antimalarial action of amodiaquine. The hydrogen bonds, which are formed by the water molecules and chlorine anions as proton acceptors, and the protonated nitrogen atoms as donors, are responsible for stability of the crystal structure.

Table 8
Results of natural population analysis (NPA) of charges

	Charges in ATChCo		Charges in AQ_100	
	Crystal	Optimized	Crystal	Optimized
C 1	-0.22567	-0.26112	-0.19909	-0.23417
C 2	0.00750	-0.01104	-0.03464	-0.04013
Cl 1	0.10138	0.11045	-0.00789	-0.00580
C 3	-0.15782	-0.21370	-0.21038	-0.25287
C 4	-0.14470	-0.18992	-0.16837	-0.21194
C 9	-0.11748	-0.11705	-0.12136	-0.11864
C 8	0.21778	0.21251	0.19118	0.18815
N 1	-0.45855	-0.50630	-0.47522	-0.47722
C 7	0.13963	0.09256	0.08713	0.04984
C 6	-0.30317	-0.34587	-0.31460	-0.34917
C 5	0.28964	0.29176	0.22968	0.23027
N 2	-0.47409	-0.56395	-0.52755	-0.60753
C 10	0.12984	0.10533	0.12741	0.11848
C 15	-0.21216	-0.21194	-0.21997	-0.24131
C 11	-0.15904	-0.20851	-0.21163	-0.24651
C 12	-0.22567	-0.28106	-0.22959	-0.27430
C 13	0.34046	0.35934	0.32256	0.33447
O 1	-0.67048	-0.69480	-0.69230	-0.71817
C 14	-0.11912	-0.14058	-0.09772	-0.12120
C 16	-0.22568	-0.27869	-0.24023	-0.27600
N 3	-0.40175	-0.45092	-0.54562	-0.54619
C 17	-0.20937	-0.26844	-0.21393	-0.26983
C 18	-0.63759	-0.73207	-0.64764	-0.69679
C 19	-0.20899	-0.26668	-0.21400	-0.26478
C 20	-0.63549	-0.73077	-0.63064	-0.71251

The conformation of amodiaquine free base in the crystal, excluding side aliphatic chain, is similar to the conformation of the cation in the dihydrochloride salt, but it is different from the conformation of amodiaquine cation in its crystalline tetrachlorocobaltate. This shows that tetrachlorocobaltate anion $[\text{CoCl}_4]^{2-}$ has significant influence on the cation conformation.

The geometry of the conjugated system consisting of the 4-[(7-chloro-4-quinolinyl)amino]phenol and quinoline moieties bridged by the trigonal nitrogen atom shows the existence of a stereoelectronic effect typical for diphenylamines.

The orientations of the side chain of the cation in both cases, i.e. amodiaquine dihydrochloride and tetrachlorocobaltate, are similar to each other but they differ from that of the free base molecule. This means that hydrogen bonds formed by the nitrogen atom, N3, determine the conformation of the side chain in all structures investigated.

The conformation of the optimized free amodiaquine base is only slightly changed in comparison to that observed in the crystal. The optimized cation has conformation more similar to that observed in the tetrachlorocobaltate salt of amodiaquine, which suggests that the lability of the cation conformation is greater than that of the free base.

The π - π stacking and also hydrogen bonds, formed by the nitrogen atoms and hydroxyl group, may be postulated as the intermolecular interactions responsible for the formation of amodiaquine complex with ferriprotoporphyrin IX or with the enzyme QR2.

7. Supplementary materials

CCDC 297105 for compound ADChM, CCDC 626826 for AQ, CCDC 626827 for AQ_100, CCDC 626825 for ATChCo contain the supplementary crystallographic data for this paper. These data can be obtained free of charge via www.ccdc.cam.ac.uk/conts/retrieving.html (or from the Cambridge Crystallographic Data Centre, 12 Union Road, Cambridge CB2 1EZ, UK; fax: C44 1223 336033; or deposit@ccdc.cam.ac.uk).

Acknowledgement

This work has been supported by grant of Polish Ministry of Education and Science, No. 1 T09A 06930

References

- [1] World Malaria Report 2005, prepared by Roll Back Malaria, World Health Organization, UNICEF.
- [2] J.J. Kwiek, T.A.J. Haystead, J. Rudolph, *Biochemistry* 43 (2004) 458.
- [3] F. Vella, G. Ferry, P. Delagrangue, J.A. Boutin, *Biochem. Pharmacol.* 71 (2005) 1.
- [4] T.J. Egan, *Exp. Opin. Ther. Patents* 11 (2) (2001) 185.
- [5] H.P. Yennawar, M.A. Viswamitra, *Curr. Sci.* 61 (1991) 39.
- [6] A. Llinàs, L. Fábrián, J.C. Burley, *Acta Crystallogr.* E62 (2006) o4196.
- [7] G.M. Sheldrick, Program for Crystal Structure Refinement, SHELXL97, University of Göttingen, Germany, 1997.
- [8] M. Nardelli, *J. Appl. Crystallogr.* 28 (1995) 659.
- [9] L.J. Farrugia, *J. Appl. Crystallogr.* 30 (1997) 565.
- [10] M.J. Frisch, G.W. Trucks, H.B. Schlegel, G.E. Scuseria, M.A. Robb, J.R. Cheeseman, J.A. Montgomery Jr., T. Vreven, K.N. Kudin, J.C. Burant, J.M. Millam, S.S. Iyengar, J. Tomasi, V. Barone, B. Mennucci, M. Cossi, G. Scalmani, N. Rega, G.A. Petersson, H. Nakatsuji, M. Hada, M. Ehara, K. Toyota, R. Fukuda, J. Hasegawa, M. Ishida, T. Nakajima, Y. Honda, O. Kitao, H. Nakai, M. Klene, X. Li, J.E. Knox, H.P. Hratchian, J.B. Cross, V. Bakken, C. Adamo, J. Jaramillo, R. Gomperts, R.E. Stratmann, O. Yazyev, A.J. Austin, R. Cammi, C. Pomelli, J.W. Ochterski, P.Y. Ayala, K. Morokuma, G.A. Voth, P. Salvador, J.J. Dannenberg, V.G. Zakrzewski, S. Dapprich, A.D. Daniels, M.C. Strain, O. Farkas, D.K. Malick, A.D. Rabuck, K. Raghavachari, J.B. Foresman, J.V. Ortiz, Q. Cui, A.G. Baboul, S. Clifford, J. Cioslowski, B.B. Stefanov, G. Liu, A. Liashenko, P. Piskorz, I. Komaromi, R.L. Martin, D.J. Fox, T. Keith, M.A. Al-Laham, C.Y. Peng, A. Nanayakkara, M. Challacombe, P. M.W. Gill, B. Johnson, W. Chen, M.W. Wong, C. Gonzalez, J.A. Pople, *Gaussian 03, Revision C.02*, Gaussian, Inc., Wallingford, CT, 2004.
- [11] A.D. Becke, *J. Chem. Phys.* 98 (1993) 5648.
- [12] C. Lee, W. Yang, R.G. Parr, *Phys. Rev. B* 37 (1988) 785.
- [13] W.J. Hehre, R. Ditchfield, J.A. Pople, *J. Chem. Phys.* 56 (1972) 2257.
- [14] A.E. Reed, R.B. Weinstock, F. Weinhold, *J. Chem. Phys.* 83 (1985) 735.
- [15] B. Lakard, G. Herlem, B. Fahys, *J. Mol. Struct. (Theochem)* 584 (2002) 15.
- [16] I. Hargittai, M. Hargittai, *Symmetry through the Eyes of a Chemist*, UCH, 1987.
- [17] G. Häfelfinger, H.-G. Mack, Z. Rappoport (Eds.), *The Chemistry of enamines*, part 1, John Wiley & Sons, New York, 1994.
- [18] I. Kortišová, M. Breza, P. Šimon, *J. Mol. Struct. (Theochem)* 723 (2005) 23.
- [19] L.B. Casabianca, C.M. Faller, A.C. de Dios, *J. Phys. Chem. A* 110 (2006) 7787.
- [20] A.C. de Dios, L.B. Casabianca, A. Kosar, P.D. Roepe, *Inorg. Chem.* 43 (2004) 8078.
- [21] L.B. Casabianca, A.C. de Dios, *J. Phys. Chem.* 108 (2004) 8505.